



1 **Variability and Uncertainty in Flux-Site Scale Net Ecosystem**
2 **Exchange Simulations Based on Machine Learning and**
3 **Remote Sensing: A Systematic Evaluation**

4 Haiyang Shi^{1,2,4,5}, Geping Luo^{1,2,3,5}, Olaf Hellwich⁶, Mingjuan Xie^{1,2,4,5}, Chen Zhang^{1,2}, Yu Zhang^{1,2}, Yuangang
5 Wang^{1,2}, Xiuliang Yuan¹, Xiaofei Ma¹, Wenqiang Zhang^{1,2,4,5}, Alishir Kurban^{1,2,3,5}, Philippe De Maeyer^{1,2,4,5} and
6 Tim Van de Voorde^{4,5}

7

8 ¹ State Key Laboratory of Desert and Oasis Ecology, Xinjiang Institute of Ecology and Geography, Chinese
9 Academy of Sciences, Urumqi, Xinjiang, 830011, China.

10 ² University of Chinese Academy of Sciences, 19 (A) Yuquan Road, Beijing, 100049, China.

11 ³ Research Centre for Ecology and Environment of Central Asia, Chinese Academy of Sciences, Urumqi, China.

12 ⁴ Department of Geography, Ghent University, Ghent 9000, Belgium.

13 ⁵ Sino-Belgian Joint Laboratory of Geo-Information, Ghent, Belgium and Urumqi, China.

14 ⁶ Department of Computer Vision & Remote Sensing, Technische Universität Berlin, 10587 Berlin, Germany.

15

16 **Correspondence to:** Geping Luo (luogp@ms.xjb.ac.cn) and Olaf Hellwich (olaf.hellwich@tu-berlin.de)

17



18 **Abstract.** Net ecosystem exchange (NEE) is an important indicator of carbon cycling in terrestrial ecosystems.
19 Many previous studies have combined flux observations, meteorological, biophysical, and ancillary predictors
20 using machine learning to simulate the site-scale NEE. However, systematic evaluation of the performance of
21 such models is limited. Therefore, we performed a meta-analysis of these NEE simulations. Total 40 such
22 studies and 178 model records were included. The impacts of various features throughout the modeling process
23 on the accuracy of the model were evaluated. Random Forests and Support Vector Machines performed better
24 than other algorithms. Models with larger time scales have lower average R-squared, especially when the time
25 scale exceeds the monthly scale. Half-hourly models (average R-squared = 0.73) were significantly more
26 accurate than daily models (average R-squared = 0.5). There are significant differences in the predictors used
27 and their impacts on model accuracy for different plant functional types (PFT). Studies at continental and global
28 scales (average R-squared = 0.37) with multiple PFTs, more sites, and a large span of years correspond to lower
29 R-squared than studies at local (average R-squared = 0.69) and regional scales (average R-squared = 0.7). Also,
30 the site-scale NEE predictions need more focus on the internal heterogeneity of the NEE dataset and the
31 matching of the training set and validation set. The results of this study may also be applicable to the prediction
32 of other carbon fluxes such as methane.

33 **1 Introduction**

34 Net ecosystem exchange (NEE) of CO₂ is an important indicator of carbon cycling in terrestrial ecosystems (Fu
35 et al., 2019), and accurate estimation of NEE is important for the development of global carbon neutral policies.
36 Although process-based models have been used for NEE simulations (Mitchell et al., 2009), their accuracy and
37 spatial resolutions of the model outputs are limited probably due to the lack of understanding and quantification
38 of complex processes. Many researchers have tried to use a data-driven approach as an alternative (Fu et al.,
39 2014; Jung et al., 2011; Tian et al., 2017; Tramontana et al., 2016), with the growth of global carbon flux
40 observations and the large amount of flux observation data being accumulated. Various machine learning
41 methods have been used to simulate NEE at the flux station scale with various predictor variables (e.g.,
42 meteorological factors, biophysical variables) incorporated for spatial and temporal mapping of NEE or
43 understanding the driving mechanisms of NEE.

44
45 To date, a synthesis evaluation of the performance of these machine learning models is still limited. Since the
46 beginning of this century, when machine learning approaches were still rarely used in geography and ecology
47 research, neural networks were already used to perform simulations and mapping of NEE in European forests
48 (Papale and Valentini, 2003). Subsequently, considerable efforts have been made by researchers to improve
49 such predictive models. Many papers have demonstrated the effectiveness of their proposed improvements by
50 comparing the accuracy of the models developed in previous studies. However, the improvements achieved in
51 these studies may be limited to smaller areas and specific conditions and may not be generalizable (Cho et al.,
52 2021; Cleverly et al., 2020; Reed et al., 2021). Through these comparisons, it remains not easy for us to
53 understand the general guidelines for selecting appropriate predictor variables and models. The effectiveness of
54 various predictors under different conditions and how to further improve model accuracy are still uncertain. We
55 should synthesize the results of models applied to different conditions and regions to gain general insights.

56



57 Many factors may affect the performance of these models, such as the predictor variables, the spatial and
58 temporal span of the observed flux data, the PFT of the flux sites, the model validation method, the machine
59 learning algorithm used, as described below:

60 a) Predictors: Various biophysical variables (Cui et al., 2021; Huemmrich et al., 2019; Zeng et al., 2020) and
61 other meteorological and environmental factors have been used in the simulation of NEE. The most
62 commonly used predictor variables include precipitation (Prec), air temperature (Ta), wind speed (Ws),
63 net/sun radiation (Rn/Rs), soil temperature (Ta), soil texture, soil moisture (SM) (Zhou et al., 2020), vapor-
64 pressure deficit (VPD) (Moffat et al., 2010; Park et al., 2018), the fraction of absorbed photosynthetically
65 active radiation (FAPAR) (Park et al., 2018; Tian et al., 2017), vegetation index (e.g., NDVI, EVI), LAI,
66 and evapotranspiration (ET) (Berryman et al., 2018). The predictor variables used vary with the natural
67 conditions and vegetation functional types of the study area. In contrast, in models that include multiple
68 plant functional types (PFT), some variables that play a significant role in the prediction of each of the
69 multiple PFTs may have higher importance. For example, growing degree days (GDD) may be a more
70 effective variable for NEE of tundra in the northern hemisphere high latitudes (Virkkala et al., 2021), while
71 measured groundwater levels may be important for wetlands (Zhang et al., 2021). Some of these predictor
72 variables are measured at flux stations (e.g., meteorological factors such as precipitation and temperature),
73 while others are extracted from reanalyzed meteorological datasets and satellite remote sensing image data
74 (e.g., vegetation indices). The spatial and temporal resolution of predictors can lead to differences in their
75 relevance to NEE observations. Most measured in situ meteorological factors have a good spatio-temporal
76 match to the observed NEE (site scale, half-hourly scale). However, the proportion of NEE explained by
77 remotely sensed biophysical covariates may depend on their spatial and temporal scales. For example, the
78 MODIS-based 8-daily NDVI data may better capture temporal variation in the relationship between NEE
79 and vegetation growth than the Landsat-based 16-daily NDVI data. In contrast, the interpretation of NEE
80 by variables such as soil texture and soil organic content (SOC), which do not have temporal dynamic
81 information, may be limited to the interpretation of spatial variability, although they are considered to be
82 important drivers of NEE. Therefore, the importance of variables obtained from NEE simulations based on
83 a data-driven approach may differ from that in process-based models as well as in the actual driving
84 mechanisms. This may be related to the spatial and temporal resolution of the predictors used and the
85 quality of the data. It is necessary to consider the spatio-temporal resolution of the data for the actual
86 biophysical variables used in the different studies in the systematic evaluation of data-driven NEE
87 simulations.

88 b) The volume of data sets, spatio-temporal heterogeneity, and validation method: The volume and spatio-
89 temporal heterogeneity of the dataset may affect model accuracy. Typically, training data with larger
90 regions, multiple sites, multiple PFTs, and longer spans of years may have a higher degree of imbalance
91 (Kaur et al., 2019; Van Hulse et al., 2007; Virkkala et al., 2021; Zeng et al., 2020). Modeling with
92 unbalanced data (where the difference between the distribution of the training and validation sets is
93 significant even if selected at random) may result in lower model accuracy. To date, the most commonly
94 used methods for validating such models include spatial (Virkkala et al., 2021), temporal (Reed et al.,
95 2021), and random (Cui et al., 2021) cross-validation. The imbalance of data between the training and
96 validation sets may affect the accuracy of the models when using these validation methods. Spatial



97 validation is used to assess the ability of the model to adapt to different regions or flux sites of different
98 PFTs, and a common method is 'leave one site out' cross-validation (Virkkala et al., 2021; Zeng et al.,
99 2020). If the data from the site left out is not covered (or partially covered) by the distribution of the
100 training dataset, the model's prediction performance at that site may be poor due to the absence of a similar
101 type in the training set. Temporal validation typically uses some years of data as training and the remaining
102 years as validation to assess the model's fitness for interannual variability. For a year that is left out (e.g. a
103 special extreme drought year which does not occur in the training set), the accuracy of the model may be
104 limited if there are no similar years (extreme drought years) in the training dataset. K-fold cross-validation
105 is commonly used in random cross-validation to assess the fitness of the model to the spatio-temporal
106 variability. In this case, different values of K may also have a significant impact on the model accuracy.
107 For example, for an unbalanced dataset, the average model accuracy obtained from a 10-fold ($K = 10$)
108 validation approach is likely to be higher than that of a 3-fold ($K = 3$) validation approach.

109 c) Machine learning algorithms used: Simulating NEE using different machine learning algorithms may
110 influence the model accuracy, which may be induced by the characteristics of these algorithms themselves
111 and the specific data distribution of the NEE training set. For example, Neural Networks can be used
112 effectively to deal with nonlinearities, while as an ensemble learning method, Random Forests can avoid
113 overfitting due to the introduction of randomness. Therefore, a comprehensive evaluation of this is
114 necessary.

115

116 In this study, to evaluate the impact of predictors and other features on model accuracy, we performed a meta-
117 analysis of papers with prediction models that combine NEE observations from flux towers, various predictors,
118 and machine learning for the data-driven NEE simulations. In addition, we also analyzed the causality of
119 multiple features in NEE simulations and the joint effects of multiple features on model accuracy using
120 Bayesian Network (BN) (a multivariate statistical analysis approach (Pearl, 1985)). The findings of this study
121 can provide some general guidance for future NEE simulations.

122 **2 Methodology**

123 **2.1 Criteria for including articles**

124 In the Scopus database, a literature query was applied to titles, abstracts, and keywords (Table 1) according to
125 Preferred Reporting Items for Systematic Reviews and Meta-Analyses (PRISMA) (Moher et al., 2009) (Fig. 1):

- 126 a) Articles were filtered for those that modeled NEE. Articles that modeled other carbon fluxes such as
127 methane flux were not included.
- 128 b) Articles that used only univariate regression rather than multiple regression were screened out.
- 129 c) Articles reported the determination coefficient (R-squared) of the validation step (Shi et al., 2021;
130 Tramontana et al., 2016; Zeng et al., 2020) as the measure of model performance. Although RMSE is also
131 often used for model accuracy assessment, its dependence on the magnitude of water flux values makes it
132 difficult to use for fair comparisons between studies.
- 133 d) Articles were published in journals with language limited to English.



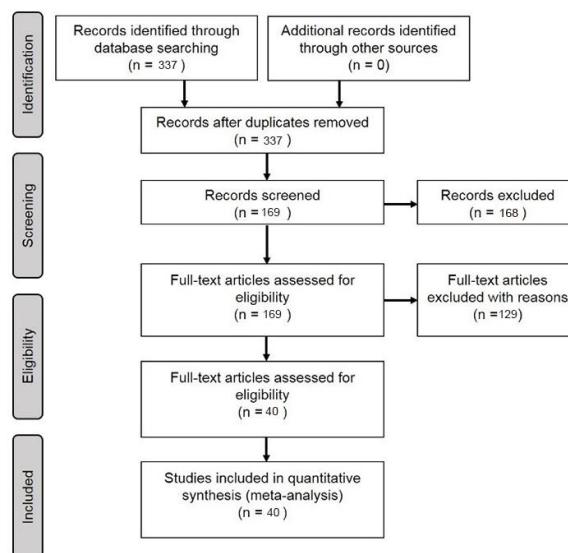
134 e) Articles were filtered for those that were published in the specific journals (Table S1) for research quality
 135 control because the data, model implements, and peer review in these journals are often more reliable.

136

137 Table 1. Article search query design: '[A1 OR A2 OR A3...] AND [B1 OR B2...] AND [C1 OR C2...]'

ID	A	B	C
1	Carbon flux	“Eddy covariance”	“machine learning”
2	CO2 flux	“Flux tower”	regress*
3	“net ecosystem exchange”		“Support Vector”
4	net ecosystem produc		“Neural Network”
5	gross primary produc		“Random Forest”
6	Carbon exchange		

138



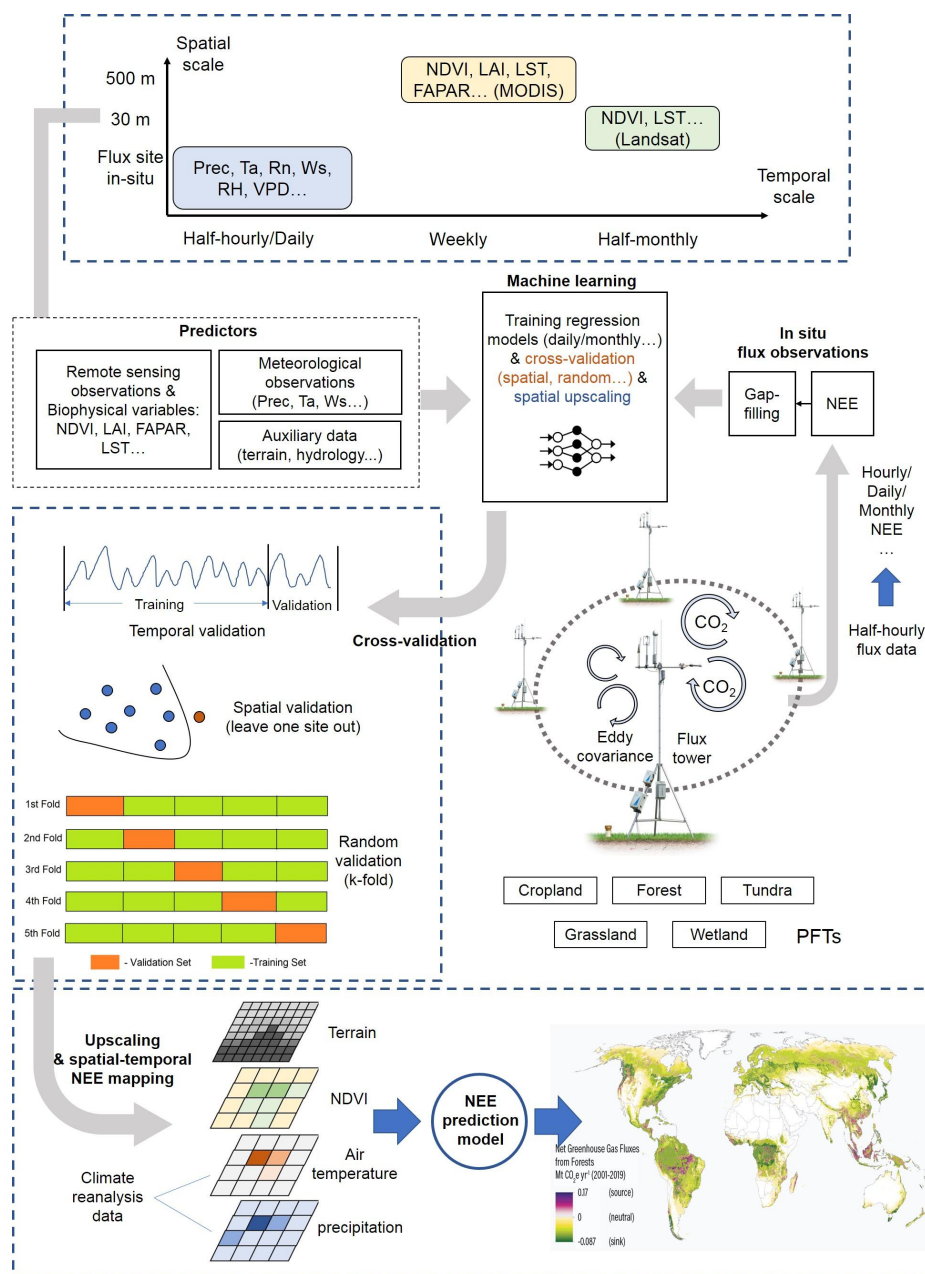
139

140 Figure 1. PRISMA-based paper filtering flowchart.

141 **2.2 Features of prediction models**

142 From the included papers, various features (Table 2) involved in the NEE modeling framework (Fig. 2) can be
 143 extracted including algorithms, modeling/validation, remote sensing data, meteorological data, biophysical data,
 144 ancillary data, and PFTs for the study area or sites. The information of R-squared (at the validation phase) and
 145 the associated model features reported in the article are considered as one data record for the formal meta-
 146 analysis. In some studies, multiple algorithms were applied to the same dataset, or models with different features
 147 were developed. In these cases, multiple data records will be documented.

148



149
 150 Figure 2. Features of the machine learning-based NEE prediction process. The flux tower photo is from
 151 <https://www.licor.com/env/support/Eddy-Covariance/videos/ec-method-02.html> (last accessed: 23rd March
 152 2022). The map in the lower part is from Harris et al., 2021.

153

154 Table 2. Description of information extracted from the included papers.

Field/Feature	Definition	Categories adopted
---------------	------------	--------------------



Id paper	Identification number of the paper (internal)	
Paper	Paper metadata	
Author/s	Name/s of author/s	
Title	Title of the paper	
Year	Year of publication	
Publication title	Name of the journal where the paper was published	
Plant functional type (PFT)	PFTs for the flux sites used	1-forest, 2-grassland, 3-cropland, 4-wetland, 5-savannah, 6-tundra and multi-PFTs
Location	More precise location (with the latitude and longitude of the center of the studied sites). Global (mainly based on FluxNet (Tramontana et al., 2016)) and continental-scale studies are not shown on the map due to the difficulty of identifying specific locations.	latitude, longitude
Algorithms	Algorithm families used in the multivariate regression	Random Forests (RF), Multiple Linear Regressions (MLR), Artificial Neural Networks (ANN), Support Vector Machines (SVM), Partial Least Squares Regression (PLSR), Generalized additive model (GAM), Boosted Regression Tree (BRT), Bayesian Additive Regression Trees (BART), Cubist, model tree ensembles (MTE).
Sites number	Number of the flux sites used	
Study area/Spatial scale	Area representatively covered by the flux sites	local (less than 100 x 100km), regional, global (continent-scale and global scale)
Temporal scale	The temporal scale of the model	half-hourly, hourly, daily, weekly, 8-daily, monthly, seasonally, yearly
Study period	The period of the data used in the model	year, growing season, daytime, spring, summer, autumn, winter
Year span	The span of years of the flux data used	
Site year	Describe the volume of total flux data with the number of sites and years aggregated.	
Cross-validation	Describe the chosen method of cross-validation.	Spatial (e.g., 'leave one site out'), temporal (e.g., 'leave one year out'), random (e.g., 'k-fold')
Training/validation	Describe the ratio of the data in training and validation sets.	



Satellite images	Describe the source of satellite images used to derive NDVI, EVI, LAI, LST, etc.	Landsat, MODIS, Hyperion (EO-1), AVHRR, IKONOS
Biophysical predictors	LAI, NDVI/EVI, evapotranspiration (ET), enhanced vegetation index (EVI), the fraction of absorbed photosynthetically active radiation/photosynthetically active radiation (FAPAR/PAR), leaf area index (LAI), etc.	Used (recorded as '1') or not used (recorded as '0')
Meteorological variables	precipitation (Prec), net radiation/solar radiation (Rn/Rs), air temperature (Ta), vapour-pressure deficit (VPD), relative humidity (RH) , etc.	Used (recorded as '1') or not used (recorded as '0')
Ancillary data	Describe the source of ancillary variables including terrain variables derived from DEM, soil texture, or hydrology-related data: soil organic content (SOC), soil texture, terrain, soil moisture/land surface water index (SM_LSWI), etc.	Used (recorded as '1') or not used (recorded as '0')
Top three variables in the ranking of importance of predictors	Describe the interpretation of the importance of variables in machine learning models.	
Accuracy measure	Accuracy measure used to assess the performance of the estimation/prediction	R-squared (in the validation phase)

155

156 2.3 Bayesian Network for analyzing joint effects

157 Based on the Bayesian network (BN), the joint impacts of multiple model features on the R-squared are
 158 analyzed. A BN can be represented by nodes (X_1, \dots, X_n) and the joint distribution (Pearl, 1985):

$$159 P(X) = P(X_1, X_2, \dots, X_n) = \prod_{i=1}^n P(X_i | pa(X_i)) \quad \#(1)$$

160 where $pa(X_i)$ is the probability of the parent node X_i . Expectation-maximization (EM) approach (Moon, 1996) is
 161 used to incorporate the collected model records and compile the BN.

162

163 Sensitivity analysis is used for the evaluation of node influence based on mutual information (MI) which is
 164 calculated as the entropy reduction of the child node resulting from changes at the parent node (Shi et al., 2020):

$$165 MI = H(Q) - H(Q|F) = \sum_q \sum_f P(q, f) \log_2 \left(\frac{P(q, f)}{P(q)P(f)} \right) \quad \#(2)$$

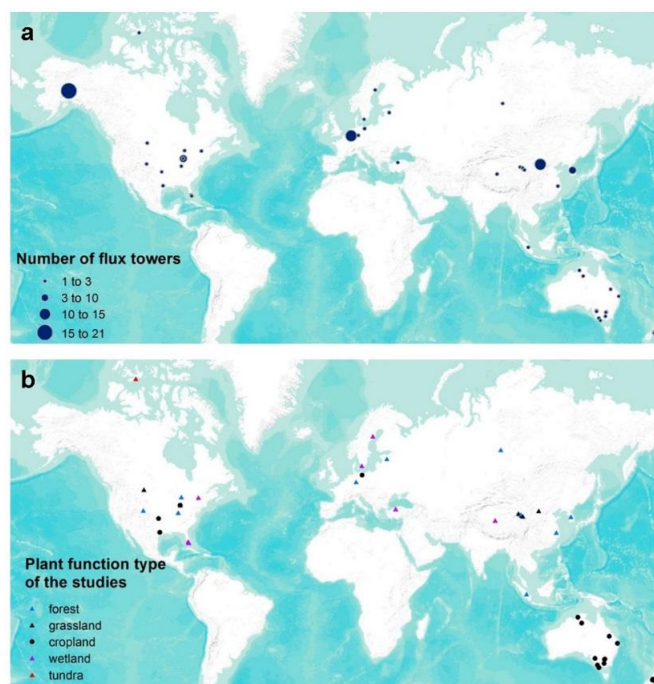
166 where H represents the entropy, Q represents the target node, F represents the set of other nodes and q and f
 167 represent the status of Q and F.



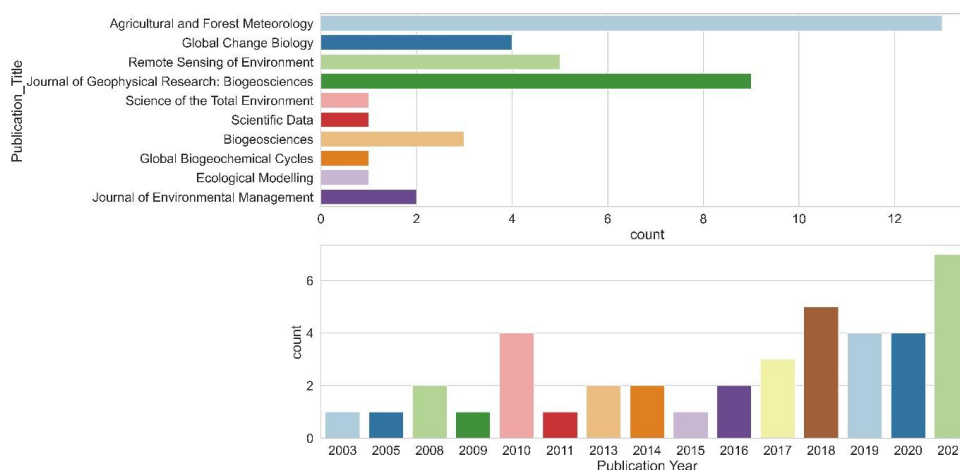
168 **3 Results**

169 **3.1 Articles included in the meta-analysis**

170 We included 40 articles (Table S2) and extracted 178 model records for the formal meta-analysis (Fig. 1). Most
171 studies were implemented in Europe, North America, Oceania, and China (Fig. 3). The number of such papers is
172 increasing recently (Fig. 4) and it shows the machine learning approach for NEE prediction has been of interest
173 to more researchers. The main journals in which these articles have been published (Fig. 4) include Remote
174 Sensing of Environment, Global Change Biology, Agricultural and Forest Meteorology, Biogeosciences, Journal
175 of Geophysical Research: Biogeosciences, etc.
176



177
178 Figure 3. Location of studies (a) included with the number of flux sites included and (b) their PFTs in the meta-
179 analysis (total 40 studies and 178 model records). Global (mainly based on FluxNet (Tramontana et al., 2016))
180 and continental-scale studies are not shown on the map due to the difficulty of identifying specific locations.
181



182

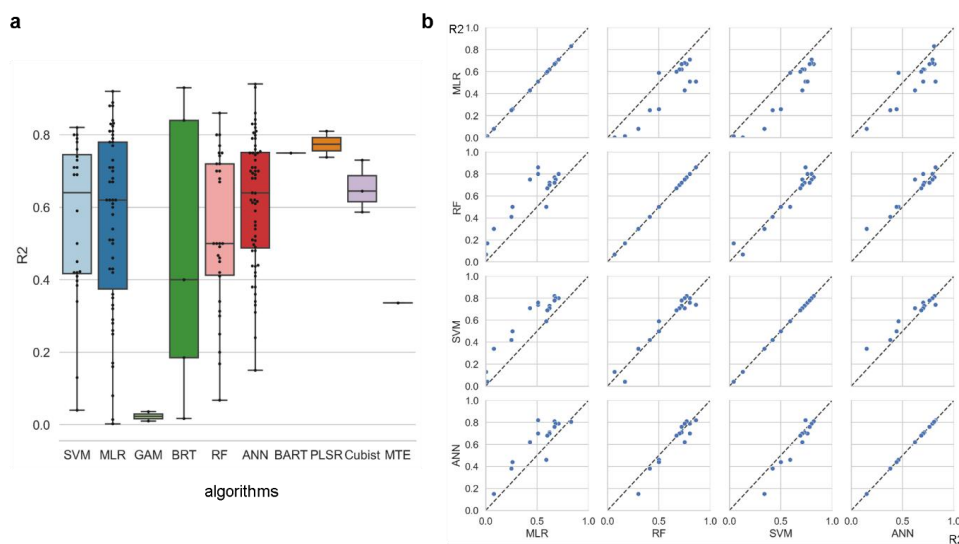
183 Figure 4. The number of studies published across journals and the total number of publications per year.

184 3.2 The formal Meta-analysis

185 We assessed the impact of the features (e.g., algorithms, study area, PFTs, amount of data, validation methods,
186 predictor variables, etc.) used in the different models based on differences of R-squared.

187 3.2.1 Algorithms

188 Among the more frequently used algorithms, ANN and SVM performed better (Fig. 5) on average across studies
189 (lightly better than RF). Unexpectedly, the cross-study average performance of the conventional MLR was not
190 worse than these three machine learning algorithms (i.e., ANN, SVM, RF). This may be because some of the
191 studies that used MLR did not divide the training and validation sets, and the R-squared of the validation set of a
192 model may be typically lower than that of the training set. On the other hand, an internal comparison of studies
193 that developed multiple models with the same training set and model features (Fig. 5) shows that RF and SVM
194 perform best when the interference of other features is reduced. Whereas ANN performed slightly worse than
195 RF and SVM, all three of them were significantly stronger than MLR. Overall, the performance of RF and SVM
196 may be similar in the NEE simulations.



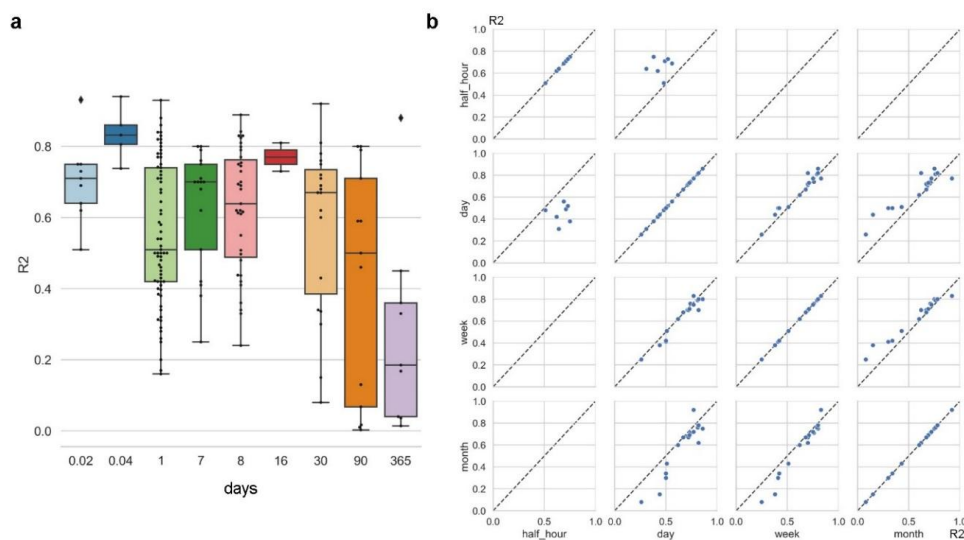
197

198 Figure 5. Differences in model accuracy (R-squared) using different algorithms across studies (a) and
199 internal comparisons of the model accuracy (R-squared) of selected pairs of algorithms within individual studies (b).

200 Regression algorithms: Random Forests (RF), Multiple Linear Regressions (MLR), Artificial Neural Networks
201 (ANN), Support Vector Machines (SVM), Partial Least Squares Regression (PLSR), Generalized additive
202 model (GAM), Boosted Regression Tree (BRT), Bayesian Additive Regression Trees (BART), Cubist, model
203 tree ensembles (MTE).

204 3.2.2 Temporal scales

205 The impact of time scale on R-squared is significant (Fig. 6), with models with larger time scales having lower
206 average R-squared, especially when the time scale exceeds the monthly scale. The most frequently used scales
207 were the daily, 8-day, and monthly scales. In studies where multiple time scales were used with other
208 characteristics being the same, we found that models with half-hourly scales were significantly more accurate
209 than models with daily scales (Fig. 6). However, the difference in accuracy between the day-scale and week-
210 scale models is small. The accuracy of models with a monthly scale is the lowest.



211

212 Figure 6. Differences in model accuracy (R-squared) at different time scales across studies (a) and
213 comparison of the model accuracy (R-squared) of selected pairs of time scales within individual
214 studies (b). Time scales: 0.02 days (half-hourly), 0.04 days (hourly), 30 days (monthly), 90 days
215 (quarterly).

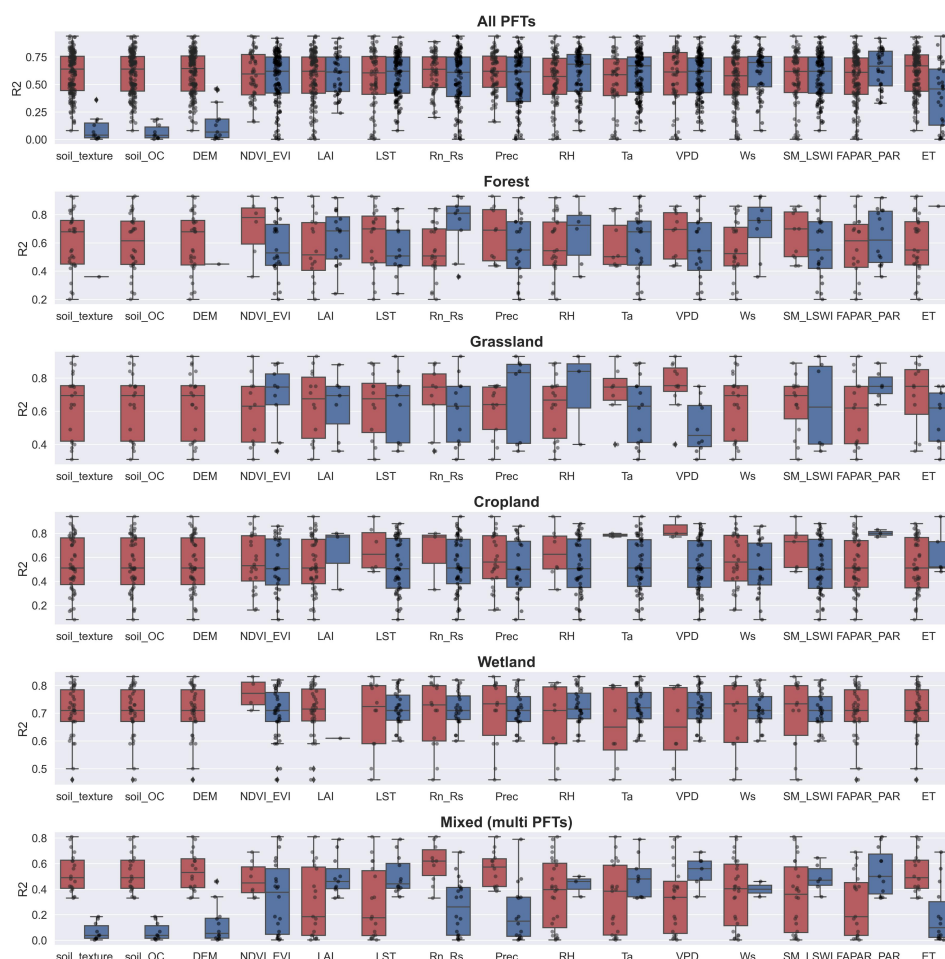
216 3.2.3 Various predictors

217 Among the commonly used predictors for NEE, there are significant differences in the predictors used and their
218 impacts on model accuracy for different PFTs (Fig. 7). Ancillary data (e.g. soil texture, soil organic content,
219 topography) that do not have temporal variability are used less frequently because they can only explain spatial
220 heterogeneity. In contrast, the biophysical variables LAI, FAPAR, and ET were used significantly less
221 frequently than NDVI/EVI, especially in the cropland and wetland types. The meteorological variables T_a ,
222 R_n/R_s , and VPD were used most frequently. For forest sites, R_n/R_s and W_s appear to be the variables that
223 significantly improve model accuracy. For grassland sites, we found that NDVI/EVI appear to be the most
224 effective, despite the small sample size. For sites in croplands and wetlands, we did not find predictor variables
225 that had a significant impact on model accuracy.

226

227 For different PFTs, the top three variables in the ranking of model importance differed (Fig. S1). SM, R_n/R_s , T_a ,
228 T_s , and VPD all showed high importance across PFTs. This suggests that the variability of measured site-scale
229 moisture and temperature conditions is important for the simulation of NEE for all PFTs. In contrast, in the
230 importance ranking, other variables such as precipitation and NDVI/EVI may not lead because of the lag in their
231 effect on NEE. And some other variables may improve model accuracy for specific PFTs such as groundwater
232 table depth (GWT) for wetland sites and growing degree days (GDD) for tundra sites.

233



234

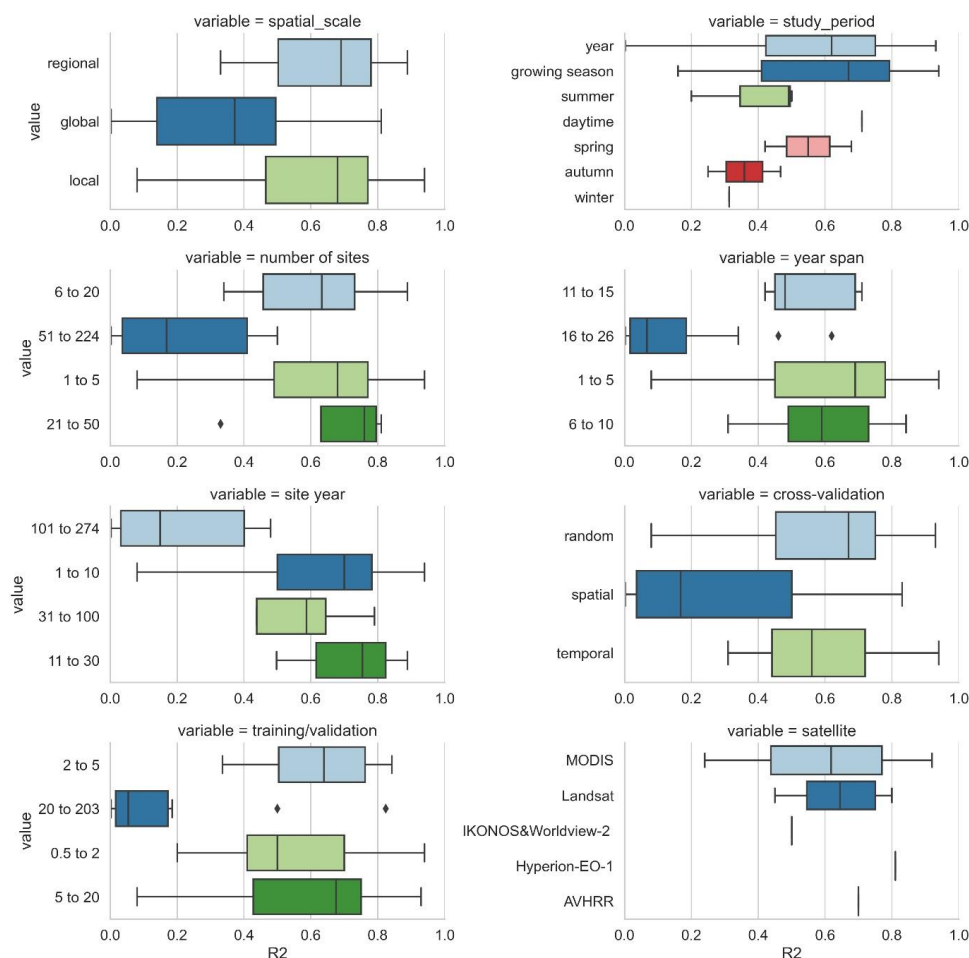
235 Figure 7. The impact of the various predictors incorporated in models of different PFTs (1-forest, 2-grassland, 3-
236 cropland, 4-wetland, 6-tundra) on R-squared. Dark blue boxes indicate that the predictor was used in the model,
237 while dark red boxes indicate that the predictor was not used. Predictors: soil organic content (Soil_OC),
238 precipitation (Prec), soil moisture/land surface water index (SM_LSWI), net radiation/solar radiation (Rn_Rs),
239 enhanced vegetation index (EVI), air temperature (Ta), vapor-pressure deficit (VPD), the fraction of absorbed
240 photosynthetically active radiation/photosynthetically active radiation (FAPAR_PAR), relative humidity (RH),
241 evapotranspiration (ET), leaf area index (LAI).

242 3.2.4 Other features

243 In addition, we evaluated other features of the model construction that may contribute to differences in model
244 accuracy (Fig. 8). Studies at continental and global scales with a large number of sites and a large span of years
245 correspond to lower R-squared than studies at local and regional scales, suggesting that studies with a large
246 number of sites across large regions are likely to have high variability in the relationship between NEE and
247 covariates and that studies at small scales are more likely to have higher model accuracy. Spatial validation



248 (usually 'leave one site out') corresponds to lower model accuracy compared to random and temporal validation.
 249 This again confirms the dominant role of heterogeneity in the relationship between NEE and covariates across
 250 sites in explaining model accuracy. This seems to be indirectly supported by the fact that a high ratio of training
 251 to validation sets corresponds to a low R-squared, as this high ratio tends to be accompanied by the use of the
 252 'leave one site out' validation approach. The accuracy of the models with a growing season period was slightly
 253 higher than that of the models with an annual period. For the satellite remote sensing data used, the models
 254 based on MODIS data with biophysical variables extracted were slightly less accurate than those based on
 255 Landsat data. For the daily scale models, Landsat data performed a little better than MODIS (Fig. S2), probably
 256 because the monitored area (approximately 100 x 100 m with a high proportion of flux footprints) of the eddy-
 257 covariance flux tower was more suitable for the use of Landsat data. MODIS data at the 500 m or 1 km scale
 258 used in the model may result in the sub-pixel heterogeneity issue and the lower representativeness than Landsat
 259 data that does not match the monitored footprint area of the flux, especially on non-homogeneous underlying
 260 surfaces (Chu et al., 2021).
 261



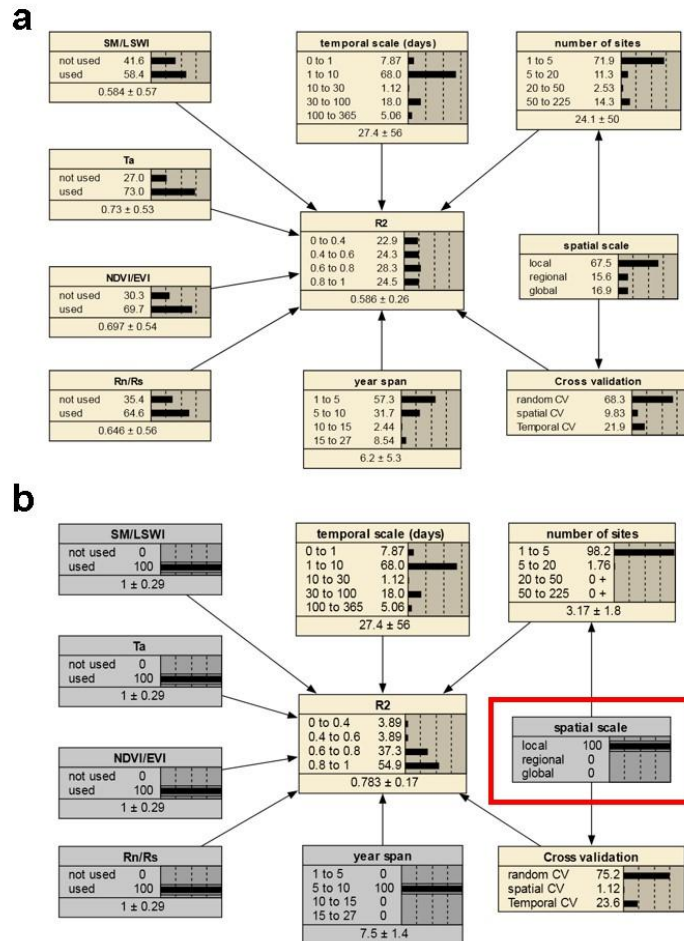
262



263 Figure 8. The impacts of other features (i.e. spatial scale, study period, number of sites, year span, site year,
264 cross-validation method, training/validation, and satellite imagery) on the model performance.

265 3.3. The joint causal impacts of multi-features based on the BN

266 We selected the features that had a more significant impact on model accuracy in the above assessment and
267 further incorporated them into the BN-based multivariate assessment to understand the joint impact of multiple
268 features on R-squared. The features incorporated included the spatial scale, the number of sites, the temporal
269 scale, the span of years, the cross-validation method, and whether some specific predictors were used. We
270 discretized the distribution of individual nodes and compiled the BN (Fig. 9.a) using records from different
271 PFTs as input. Sensitivity analysis of the R-squared node (Fig. 10) showed that R-squared was most sensitive to
272 'year span', cross-validation method, Rn/Rs, and time scale under multi-feature control. In the forest and
273 cropland types, R-squared is more sensitive to Rn/Rs, while in the wetland type it is more sensitive to SM/LSWI
274 and Ta. The sensitivity of R-squared to 'year span' was much higher in the cropland type compared to the other
275 PFTs, which may suggest that the interannual variability in the NEE simulations of the cropland type is higher
276 due to potential interannual variability of the planting structure and irrigation practices. For the cropland type,
277 differences in the phenology, harvesting, and irrigation (water volume and frequency) in different years can lead
278 to significant inter-annual differences in NEE simulations. Subsequently, using the constructed BN (with the
279 empirical information in previous studies incorporated), for new studies we can instructively infer the
280 probability distribution of the possible R-squared (Fig. 9.b) with some model features predetermined. In
281 previous studies, spatio-temporal mapping of NEE based on statistical models has often lacked accuracy
282 assessment since there are no grid-scale NEE observations, and this BN may have the potential to be used to
283 validate the accuracy (R-squared) of the NEE time series output of the grid-scale (i.e. inferring possible R-
284 squared from model features, where the output of the grid-scale is considered to be of the form 'leave one site
285 out').



286

287 Figure 9. The joint effects of multiple features on the R-squared based on the BN with all records input (a) and

288 the inference on the probability distribution of R-squared based on the BN with the status of some nodes

289 determined (b). The values before and after the “±” indicate the mean and standard deviation of the distribution,

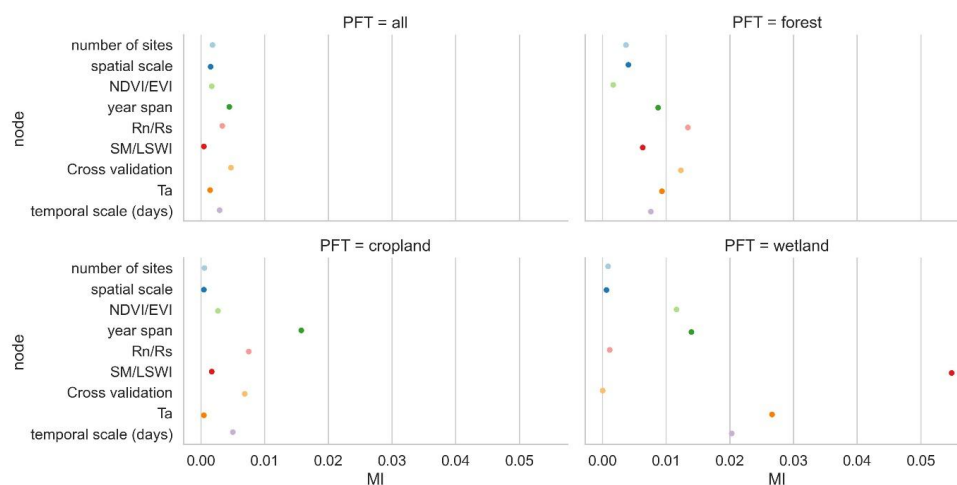
290 respectively. The gray boxes indicate that the status of the nodes has been determined. In panel (b), specific

291 values of parent nodes such as ‘spatial scale’ are determined (shown in the red box), leading to an increase in the

292 expected R-squared compared to the average scenario of the panel (a) (as inferred from the posterior conditional

293 probabilities with the status of the node ‘spatial scale’ are determined as ‘local’).

294



295

296 Figure 10. The sensitivity analysis of the R-squared node to other nodes based on the mutual information (MI)
297 across PFTs. ‘Cross-validation’ is the cross-validation method including spatial, temporal, and random cross-
298 validation.

299 4 Discussions

300 Many studies have evaluated the incorporation of various predictors and model features using machine learning
301 for improving the site-scale NEE predictions (Jung et al., 2011; Tramontana et al., 2016; Zeng et al., 2020). A
302 comprehensive evaluation of these studies to provide definitive guidance on the selection of features in NEE
303 prediction modeling is limited. This study fills the research gap with a meta-analysis of the literature through
304 statistics on the accuracy and performance of models. Machine learning-based NEE simulations and predictions
305 still suffer from high uncertainty. By better understanding the expected improvements that can be achieved
306 through the inclusion of different features, we can identify priorities for the consideration of different features in
307 modeling efforts and avoid operations decreasing model accuracy.

308 4.1 Challenges in the site-scale NEE simulation and implications for other carbon flux simulations

309 In the above analysis, we found that the effect of the time scale of the model is significant. This suggests that we
310 should be careful in determining the time scale of the model to consider whether the predictor variables used
311 will work at this time scale. Larger time scales correspond to lower model accuracy, possibly related to the fact
312 that some small-time-scale relations between NEE and covariates (especially meteorological variables) are
313 smoothed. In addition, the impacts of lagged effects of covariates are not considered in most models, which may
314 underestimate the degree of explanation of NEE for some predictor variables (e.g. precipitation). Most of the
315 machine learning-based models use only the average Ta and do not take into account the maximum temperature,
316 minimum temperature, daily difference in temperature, etc., as in the process-based ecological models. This
317 suggests that the inclusion of different temporal characteristics of individual variables in machine learning-based
318 NEE prediction models may be inadequate.

319



320 The impact of differences in the various satellite images on model accuracy and performance is limited.
321 Performance of studies using Landsat data is slightly better than MODIS probably because of the higher spatial
322 resolution although the 8-daily (or a smaller daily scale) timescale of MODIS may have a positive effect on the
323 accuracy improvement compared to the 16-daily timescale of Landsat. For studies using MODIS data, an
324 excessively large extraction area of remote sensing data (e.g., 2 km x 2 km) may be inappropriate. In the non-
325 homogeneous underlying conditions, the agreement of the area of flux footprints with the scale of the predictors
326 should be considered in the extraction of the predictor variables in various PFTs (Chu et al., 2021). Since few of
327 the studies included in this meta-analysis considered the effect of variation in flux footprint, this feature was
328 difficult to consider in this study, but its influence should still be further investigated in future studies with flux
329 footprints calculated (Kljun et al., 2015) and the factors around the flux site (Walther et al., 2021) that affect the
330 flux footprint are incorporated. In particular, for models with time scales smaller than one day (e.g. half-hourly
331 models), the 8-daily and 16-daily biophysical variable data obtained from satellite remote sensing are difficult to
332 explain the temporal variation in the sub-daily NEE. Therefore, for models at small time scales (i.e. half-hourly,
333 hourly, daily scale models), in situ meteorological variables may be more important. The inclusion of some
334 ancillary variables (e.g. soil texture, topographic variables) with no temporal dynamic information may be
335 ineffective unless many sites are included in the model and the spatial variability of the ancillary variables for
336 these sites is sufficiently large (Virkkala et al., 2021).

337
338 In addition to the time scale of the models, the most significant differences in model accuracy and performance
339 were found in the heterogeneity within the NEE dataset and the match of the training set and validation set.
340 Often NEE simulations can achieve high accuracy in local studies, where the main factor negatively affecting
341 model accuracy may be the interannual variability in the relationship between NEE and covariates. However,
342 the complexity may increase when the dataset contains a large study area, many sites, PFTs, and year spans.
343 Under this condition, the accuracy of the model in the 'leave one site out' validation may be more dependent on
344 the correlation and match between the training and validation sets. When the model is applied to an outlier site
345 (of which the NEE, covariates, and their relationship are very different compared with the remaining sites), it
346 appears to be difficult to achieve a high prediction accuracy. If we further upscale the prediction model to large
347 spatial and temporal scales, the uncertainties involved may be difficult to assess (Zeng et al., 2020). We can
348 only infer the possible model accuracy based on the similarity of the distribution of predictors in the predicted
349 grid to that of the existing sites in the model. In the upscaling process, coarse-resolution reanalysis
350 meteorological data are often used as an alternative for site-scale meteorological predictors. However, most
351 studies did not assess in detail the possible errors associated with spatial mismatches in this operation.

352
353 In summary, the site-scale NEE predictions may require more focus on the internal heterogeneity of the NEE
354 dataset and the matching of the training set and validation set, and also require a better understanding of the
355 influence of different scales of the same variable (e.g. site-scale precipitation and grid-scale precipitation in the
356 reanalysis meteorological data) across modeling and upscaling steps. For the prediction of other carbon fluxes
357 such as methane fluxes (in the same framework as the NEE predictions), the results of this study may also be
358 partially applicable, although there may be significant differences in the use of specific predictors (Peltola et al.,
359 2019). With fewer possible PFTs (methane flux stations are mostly located in wetlands), methane flux



360 predictions are likely to be less complex than current NEE predictions with multiple PFTs included. However,
361 studies using machine learning for methane flux modeling are currently scarce and may not be sufficient for
362 meta-analysis.

363 4.2 Uncertainties

364 The uncertainties in this analysis may include:

- 365 a) Publication bias and weighting: Publication bias is not refined due to the limitations of the number of
366 articles that can be included. Meta-analyses often measure the quality of journals and the data availability
367 (Borenstein et al., 2011; Field and Gillett, 2010) to determine the weighting among the literature in a
368 comprehensive assessment. However, a high proportion of the articles in this study did not make flux
369 observations publicly available or share the NEE prediction models developed. Furthermore, meta-analysis
370 studies in other fields typically measure the impact of papers by evidence/data volume, and the variance of
371 the evaluated effects (Adams et al., 1997; Don et al., 2011; Liu et al., 2018). However, in this study,
372 because no convincing method is found to quantify the weights of results from included articles, some
373 features (e.g. the number of flux sites, the span of years) were directly assessed rather than used to
374 determine the weights of the articles.
- 375 b) Limitations of the criteria for inclusion in the literature: in the model accuracy-based evaluation, we
376 selected only literature that developed multiple regression models. Potentially valuable information from
377 univariate regression models was not included. In addition, only papers in high-quality English journals
378 were included in this study to control for possible errors due to publication bias. However, many studies
379 that fit this theme may have been published in other languages or other journals.
- 380 c) Independence between features: There is the covariance between some of the features being evaluated (e.g.
381 the non-independence between some predictors), which may affect the assessment of the impact of
382 individual features on the accuracy of the model. The sample size collected in this study (178 records in
383 total) is not very large. The uncertainty in the findings may lead to a potentially biased understanding of
384 such studies due to the many factors that affect the accuracy of the model. This also suggests that more
385 future efforts should be devoted to the comprehensive evaluation and summarization of NEE simulations.

386
387 Additionally, there are still other potential factors not considered by this study such as the uncertainty of climate
388 data (site vs reanalysis), footprint matching between site and satellite images, etc. Overall, although the
389 quantitative results of this study should be used with caution, they still have positive implications for guiding
390 future such studies.

391 5 Conclusion

392 We performed a meta-analysis of the site-scale NEE simulations combining in situ flux observations,
393 meteorological, biophysical, and ancillary predictors, and machine learning. The impacts of various features
394 throughout the modeling process on the accuracy of the model were evaluated. The main findings of this study
395 include:

- 396 1. RF and SVM performed better than other evaluated algorithms.



- 397 2. The impact of time scale on model performance is significant. Models with larger time scales have lower
398 average R-squared, especially when the time scale exceeds the monthly scale. Models with half-hourly
399 scales (average R-squared = 0.73) were significantly more accurate than models with daily scales (average
400 R-squared = 0.5).
- 401 3. Among the commonly used predictors for NEE, there are significant differences in the predictors used and
402 their impacts on model accuracy for different PFTs.
- 403 4. It is necessary to focus on the potential imbalance between the training and validation sets in NEE
404 simulations. Studies at continental and global scales (average R-squared = 0.37) with multiple PFTs, more
405 sites, and a large span of years correspond to lower R-squared than studies at local (average R-squared =
406 0.69) and regional scales (average R-squared = 0.7).
- 407



408 **Acknowledgments**

409 This research was supported by the National Natural Science Foundation of China (Grant No. U1803243), the
410 Key projects of the Natural Science Foundation of Xinjiang Autonomous Region (Grant No. 2022D01D01), the
411 Strategic Priority Research Program of the Chinese Academy of Sciences (Grant No. XDA20060302), and
412 High-End Foreign Experts Project.

413 **Contributions**

414 H.S and G.L initiated this research and were responsible for the integrity of the work as a whole. H.S performed
415 formal analysis, calculations and drafted the manuscript. H.S, G.L, X.M, X.Y, Y.W, W.Z, M.X, C.Z, and Y.Z
416 were responsible for the data collection and analysis. G.L, P.D.M, T.V.D.V, O.H, and A.K contributed to
417 resources and financial support.

418 **Competing interests**

419 The authors declare that they have no conflict of interest.

420 **Data availability**

421 The data used in this study can be accessed by contacting the first author (shihaiyang16@mails.ucas.ac.cn)
422 based on reasonable request.

423 **Code availability**

424 The code used in this study can be accessed by contacting the first author (shihaiyang16@mails.ucas.ac.cn)
425 based on reasonable request.

426

427



428 **References**

- 429 Adams, D. C., Gurevitch, J., and Rosenberg, M. S.: Resampling tests for meta - analysis of ecological
430 data, *Ecology*, 78, 1277–1283, 1997.
- 431 Berryman, E. M., Vanderhoof, M. K., Bradford, J. B., Hawbaker, T. J., Henne, P. D., Burns, S. P.,
432 Frank, J. M., Birdsey, R. A., and Ryan, M. G.: Estimating Soil Respiration in a Subalpine Landscape
433 Using Point, Terrain, Climate, and Greenness Data, 123, 3231–3249,
434 <https://doi.org/10.1029/2018JG004613>, 2018.
- 435 Borenstein, M., Hedges, L. V., Higgins, J. P., and Rothstein, H. R.: *Introduction to meta-analysis*,
436 John Wiley & Sons, 2011.
- 437 Cho, S., Kang, M., Ichii, K., Kim, J., Lim, J.-H., Chun, J.-H., Park, C.-W., Kim, H. S., Choi, S.-W.,
438 Lee, S.-H., Indrawati, Y. M., and Kim, J.: Evaluation of forest carbon uptake in South Korea using the
439 national flux tower network, remote sensing, and data-driven technology, 311,
440 <https://doi.org/10.1016/j.agrformet.2021.108653>, 2021.
- 441 Chu, H., Luo, X., Ouyang, Z., Chan, W. S., Dengel, S., Biraud, S. C., Torn, M. S., Metzger, S.,
442 Kumar, J., Arain, M. A., Arkebauer, T. J., Baldocchi, D., Bernacchi, C., Billesbach, D., Black, T. A.,
443 Blanken, P. D., Bohrer, G., Bracho, R., Brown, S., Brunzell, N. A., Chen, J., Chen, X., Clark, K.,
444 Desai, A. R., Duman, T., Durden, D., Fares, S., Forbrich, I., Gamon, J. A., Gough, C. M., Griffis, T.,
445 Helbig, M., Hollinger, D., Humphreys, E., Ikawa, H., Iwata, H., Ju, Y., Knowles, J. F., Knox, S. H.,
446 Kobayashi, H., Kolb, T., Law, B., Lee, X., Litvak, M., Liu, H., Munger, J. W., Noormets, A., Novick,
447 K., Oberbauer, S. F., Oechel, W., Oikawa, P., Papuga, S. A., Pendall, E., Prajapati, P., Prueger, J.,
448 Quinton, W. L., Richardson, A. D., Russell, E. S., Scott, R. L., Starr, G., Staebler, R., Stoy, P. C.,
449 Stuart-Haëntjens, E., Sonnentag, O., Sullivan, R. C., Suyker, A., Ueyama, M., Vargas, R., Wood, J. D.,
450 and Zona, D.: Representativeness of Eddy-Covariance flux footprints for areas surrounding
451 AmeriFlux sites, *Agricultural and Forest Meteorology*, 301–302, 108350,
452 <https://doi.org/10.1016/j.agrformet.2021.108350>, 2021.
- 453 Cleverly, J., Vote, C., Isaac, P., Ewenz, C., Harahap, M., Beringer, J., Campbell, D. I., Daly, E.,
454 Eamus, D., He, L., Hunt, J., Grace, P., Hutley, L. B., Laubach, J., McCaskill, M., Rowlings, D.,
455 Rutledge Jonker, S., Schipper, L. A., Schroder, I., Teodosio, B., Yu, Q., Ward, P. R., Walker, J. P.,
456 Webb, J. A., and Grover, S. P. P.: Carbon, water and energy fluxes in agricultural systems of
457 Australia and New Zealand, 287, <https://doi.org/10.1016/j.agrformet.2020.107934>, 2020.
- 458 Cui, X., Goff, T., Cui, S., Menefee, D., Wu, Q., Rajan, N., Nair, S., Phillips, N., and Walker, F.:
459 Predicting carbon and water vapor fluxes using machine learning and novel feature ranking
460 algorithms, 775, <https://doi.org/10.1016/j.scitotenv.2021.145130>, 2021.
- 461 Don, A., Schumacher, J., and Freibauer, A.: Impact of tropical land-use change on soil organic carbon
462 stocks – a meta-analysis, 17, 1658–1670, <https://doi.org/10.1111/j.1365-2486.2010.02336.x>, 2011.
- 463 Field, A. P. and Gillett, R.: How to do a meta - analysis, *British Journal of Mathematical and*
464 *Statistical Psychology*, 63, 665–694, 2010.
- 465 Fu, D., Chen, B., Zhang, H., Wang, J., Black, T. A., Amiro, B., Bohrer, G., Bolstad, P., Coulter, R.,
466 Rahman, F., Dunn, A., Harry, M., Meyers, T., and Verma, S.: Estimating landscape net ecosystem
467 exchange at high spatial-temporal resolution based on Landsat data, an improved upscaling model
468 framework, and eddy covariance flux measurements, 141, 90–104,
469 <https://doi.org/10.1016/j.rse.2013.10.029>, 2014.



- 470 Fu, Z., Stoy, P. C., Poulter, B., Gerken, T., Zhang, Z., Wakbulcho, G., and Niu, S.: Maximum carbon
471 uptake rate dominates the interannual variability of global net ecosystem exchange, 25, 3381–3394,
472 <https://doi.org/10.1111/gcb.14731>, 2019.
- 473 Harris, N. L., Gibbs, D. A., Baccini, A., Birdsey, R. A., de Bruin, S., Farina, M., Fatoyinbo, L.,
474 Hansen, M. C., Herold, M., Houghton, R. A., Potapov, P. V., Suarez, D. R., Roman-Cuesta, R. M.,
475 Saatchi, S. S., Slay, C. M., Turubanova, S. A., and Tyukavina, A.: Global maps of twenty-first
476 century forest carbon fluxes, *Nat. Clim. Chang.*, 11, 234–240, <https://doi.org/10.1038/s41558-020-00976-6>, 2021.
- 478 Huemmrich, K. F., Campbell, P., Landis, D., and Middleton, E.: Developing a common globally
479 applicable method for optical remote sensing of ecosystem light use efficiency, 230,
480 <https://doi.org/10.1016/j.rse.2019.05.009>, 2019.
- 481 Jung, M., Reichstein, M., Margolis, H. A., Cescatti, A., Richardson, A. D., Arain, M. A., Arneeth, A.,
482 Bernhofer, C., Bonal, D., Chen, J., Gianelle, D., Gobron, N., Kiely, G., Kutsch, W., Lasslop, G., Law,
483 B. E., Lindroth, A., Merbold, L., Montagnani, L., Moors, E. J., Papale, D., Sottocornola, M., Vaccari,
484 F., and Williams, C.: Global patterns of land-atmosphere fluxes of carbon dioxide, latent heat, and
485 sensible heat derived from eddy covariance, satellite, and meteorological observations, 116,
486 <https://doi.org/10.1029/2010JG001566>, 2011.
- 487 Kaur, H., Pannu, H. S., and Malhi, A. K.: A Systematic Review on Imbalanced Data Challenges in
488 Machine Learning: Applications and Solutions, *ACM Comput. Surv.*, 52, 79:1-79:36,
489 <https://doi.org/10.1145/3343440>, 2019.
- 490 Kljun, N., Calanca, P., Rotach, M. W., and Schmid, H. P.: A simple two-dimensional parameterisation
491 for Flux Footprint Prediction (FFP), 8, 3695–3713, <https://doi.org/10.5194/gmd-8-3695-2015>, 2015.
- 492 Liu, Q., Zhang, Y., Liu, B., Amonette, J. E., Lin, Z., Liu, G., Ambus, P., and Xie, Z.: How does
493 biochar influence soil N cycle? A meta-analysis, *Plant and soil*, 426, 211–225, 2018.
- 494 Mitchell, S., Beven, K., and Freer, J.: Multiple sources of predictive uncertainty in modeled estimates
495 of net ecosystem CO₂ exchange, *Ecological Modelling*, 220, 3259–3270,
496 <https://doi.org/10.1016/j.ecolmodel.2009.08.021>, 2009.
- 497 Moffat, A. M., Beckstein, C., Churkina, G., Mund, M., and Heimann, M.: Characterization of
498 ecosystem responses to climatic controls using artificial neural networks, 16, 2737–2749,
499 <https://doi.org/10.1111/j.1365-2486.2010.02171.x>, 2010.
- 500 Moher, D., Liberati, A., Tetzlaff, J., Altman, D. G., and Prisma Group: Preferred reporting items for
501 systematic reviews and meta-analyses: the PRISMA statement, *PLoS medicine*, 6, e1000097, 2009.
- 502 Moon, T. K.: The expectation-maximization algorithm, 13, 47–60, 1996.
- 503 Papale, D. and Valentini, R.: A new assessment of European forests carbon exchanges by eddy fluxes
504 and artificial neural network spatialization, 9, 525–535, <https://doi.org/10.1046/j.1365-2486.2003.00609.x>, 2003.
- 506 Park, S.-B., Knohl, A., Lucas-Moffat, A. M., Migliavacca, M., Gerbig, C., Vesala, T., Peltola, O.,
507 Mammarella, I., Kolle, O., Lavrič, J. V., Prokushkin, A., and Heimann, M.: Strong radiative effect
508 induced by clouds and smoke on forest net ecosystem productivity in central Siberia, 250–251, 376–
509 387, <https://doi.org/10.1016/j.agrformet.2017.09.009>, 2018.



- 510 Pearl, J.: Bayesian networks: A model of self-activated memory for evidential reasoning, in:
511 Proceedings of the 7th Conference of the Cognitive Science Society, University of California, Irvine,
512 CA, USA, 15–17, 1985.
- 513 Peltola, O., Vesala, T., Gao, Y., Rätty, O., Alekseychik, P., Aurela, M., Chojnicki, B., Desai, A. R.,
514 Dolman, A. J., Euskirchen, E. S., Friborg, T., Göckede, M., Helbig, M., Humphreys, E., Jackson, R.
515 B., Jocher, G., Joos, F., Klatt, J., Knox, S. H., Kowalska, N., Kutzbach, L., Lienert, S., Lohila, A.,
516 Mammarella, I., Nadeau, D. F., Nilsson, M. B., Oechel, W. C., Peichl, M., Pypker, T., Quinton, W.,
517 Rinne, J., Sachs, T., Samson, M., Schmid, H. P., Sonnentag, O., Wille, C., Zona, D., and Aalto, T.:
518 Monthly gridded data product of northern wetland methane emissions based on upscaling eddy
519 covariance observations, 11, 1263–1289, <https://doi.org/10.5194/essd-11-1263-2019>, 2019.
- 520 Reed, D. E., Poe, J., Abraha, M., Dahlin, K. M., and Chen, J.: Modeled Surface-Atmosphere Fluxes
521 From Paired Sites in the Upper Great Lakes Region Using Neural Networks, 126,
522 <https://doi.org/10.1029/2021JG006363>, 2021.
- 523 Shi, H., Luo, G., Zheng, H., Chen, C., Bai, J., Liu, T., Ochege, F. U., and De Maeyer, P.: Coupling the
524 water-energy-food-ecology nexus into a Bayesian network for water resources analysis and
525 management in the Syr Darya River basin, *Journal of Hydrology*, 581, 124387,
526 <https://doi.org/10.1016/j.jhydrol.2019.124387>, 2020.
- 527 Shi, H., Hellwich, O., Luo, G., Chen, C., He, H., Ochege, F. U., Van de Voorde, T., Kurban, A., and
528 de Maeyer, P.: A global meta-analysis of soil salinity prediction integrating satellite remote sensing,
529 soil sampling, and machine learning, 1–15, <https://doi.org/10.1109/TGRS.2021.3109819>, 2021.
- 530 Tian, X., Yan, M., van der Tol, C., Li, Z., Su, Z., Chen, E., Li, X., Li, L., Wang, X., Pan, X., Gao, L.,
531 and Han, Z.: Modeling forest above-ground biomass dynamics using multi-source data and
532 incorporated models: A case study over the qilian mountains, 246, 1–14,
533 <https://doi.org/10.1016/j.agrformet.2017.05.026>, 2017.
- 534 Tramontana, G., Jung, M., Schwalm, C. R., Ichii, K., Camps-Valls, G., Ráduly, B., Reichstein, M.,
535 Arain, M. A., Cescatti, A., Kiely, G., Merbold, L., Serrano-Ortiz, P., Sickert, S., Wolf, S., and Papale,
536 D.: Predicting carbon dioxide and energy fluxes across global FLUXNET sites with regression
537 algorithms, 13, 4291–4313, <https://doi.org/10.5194/bg-13-4291-2016>, 2016.
- 538 Van Hulse, J., Khoshgoftaar, T. M., and Napolitano, A.: Experimental perspectives on learning from
539 imbalanced data, in: Proceedings of the 24th international conference on Machine learning, New York,
540 NY, USA, 935–942, <https://doi.org/10.1145/1273496.1273614>, 2007.
- 541 Virkkala, A.-M., Aalto, J., Rogers, B. M., Tagesson, T., Treat, C. C., Natali, S. M., Watts, J. D., Potter,
542 S., Lehtonen, A., Mauritz, M., Schuur, E. A. G., Kochendorfer, J., Zona, D., Oechel, W., Kobayashi,
543 H., Humphreys, E., Goeckede, M., Iwata, H., Lafleur, P. M., Euskirchen, E. S., Bokhorst, S.,
544 Marushchak, M., Martikainen, P. J., Elberling, B., Voigt, C., Biasi, C., Sonnentag, O., Parmentier, F.-
545 J. W., Ueyama, M., Celis, G., St.Louis, V. L., Emmerton, C. A., Peichl, M., Chi, J., Järveoja, J.,
546 Nilsson, M. B., Oberbauer, S. F., Torn, M. S., Park, S.-J., Dolman, H., Mammarella, I., Chae, N.,
547 Poyatos, R., López-Blanco, E., Christensen, T. R., Kwon, M. J., Sachs, T., Holl, D., and Luoto, M.:
548 Statistical upscaling of ecosystem CO₂ fluxes across the terrestrial tundra and boreal domain:
549 Regional patterns and uncertainties, 27, 4040–4059, <https://doi.org/10.1111/gcb.15659>, 2021.
- 550 Walther, S., Besnard, S., Nelson, J. A., El-Madany, T. S., Migliavacca, M., Weber, U., Ermida, S. L.,
551 Brümmer, C., Schrader, F., Prokushkin, A. S., Panov, A. V., and Jung, M.: Technical note: A view
552 from space on global flux towers by MODIS and Landsat: The FluxnetEO dataset, 1–40,
553 <https://doi.org/10.5194/bg-2021-314>, 2021.



- 554 Zeng, J., Matsunaga, T., Tan, Z.-H., Saigusa, N., Shirai, T., Tang, Y., Peng, S., and Fukuda, Y.:
555 Global terrestrial carbon fluxes of 1999–2019 estimated by upscaling eddy covariance data with a
556 random forest, 7, <https://doi.org/10.1038/s41597-020-00653-5>, 2020.
- 557 Zhang, C., Brodylo, D., Sirianni, M. J., Li, T., Comas, X., Douglas, T. A., and Starr, G.: Mapping
558 CO₂ fluxes of cypress swamp and marshes in the Greater Everglades using eddy covariance
559 measurements and Landsat data, 262, <https://doi.org/10.1016/j.rse.2021.112523>, 2021.
- 560 Zhou, Y., Li, X., Gao, Y., He, M., Wang, M., Wang, Y., Zhao, L., and Li, Y.: Carbon fluxes response
561 of an artificial sand-binding vegetation system to rainfall variation during the growing season in the
562 Tengger Desert, 266, <https://doi.org/10.1016/j.jenvman.2020.110556>, 2020.
- 563